Dog-bone versus Gaussian gigacycle fatigue specimens for size effect evaluation

A. Tridello, D.S. Paolino, G. Chiandussi, M. Rossetto
Department of Aerospace and Mechanical Engineering, Politecnico di Torino, Turin (Italy)
andrea.tridello@polito.it

ABSTRACT. Gigacycle fatigue properties of materials are strongly affected by the specimen risk volume (region subjected to a stress amplitude above the 90% of the maximum stress). Gigacycle fatigue tests, performed with ultrasonic fatigue testing machines, are commonly carried out by using hourglass shaped specimens with a small risk volume. The adoption of traditional dog-bone specimens allows for increasing the risk volume, but the increment is however limited. In order to obtain larger risk volumes, a new specimen shape is proposed (*Gaussian specimen*). The dog-bone and the Gaussian specimens are compared through Finite Element Analyses. The range of applicability of the two different specimens in terms of available risk volume and stress concentration effects due to the cross section variation is determined. Finally, the Finite Element model is validated experimentally by means of strain gages measurements.

SOMMARIO. Le proprietà dei materiali nel campo della fatica gigaciclica sono fortemente influenzate dal volume di rischio del provino (volume di materiale soggetto a una tensione superiore al 90 % della tensione massima). Le prove di fatica gigaciclica, realizzate utilizzando macchine di prova ad ultrasuoni, sono comunemente condotte utilizzando provini di tipo Hourglass con bassi volumi di rischio. L'uso di provini di tipo dog-bone permette di incrementare il volume di rischio, ma l'incremento è comunque limitato. Nel presente articolo viene proposto un nuovo profilo (*provino Gaussiano*) per aumentare ulteriormente il volume di rischio. Provini di tipo dog-bone e Gaussiano sono confrontati tramite un'analisi agli elementi finiti. Il campo di applicabilità dei due tipi di provini è determinato in termini di volume rischio reale e di fattore di concentrazione delle tensioni. Infine, attraverso misurazioni estensimetriche, il modello è anche stato validato sperimentalmente.

KEYWORDS. Very-high-cycle fatigue; Ultrasonic testing machine; Risk volume; Wave propagation equations; Stress concentration factor

INTRODUCTION

In recent years, the interest in gigacycle fatigue behaviour of metallic materials (up to 10^{10} cycles) is significantly increased. Design requirements in specific industrial fields (aerospace, mechanical and energy industry) for structural components characterized by even larger fatigue lives (gigacycle fatigue) lead to a more detailed investigation on material properties in the gigacycle regime.

Experimental results, obtained by using testing machines working in resonance conditions and capable of reaching a loading frequency equal to 20 kHz (ultrasound), have shown that specimens may fail also at levels of stress amplitude below the conventional fatigue limit [1]. It has been found that failures are generally due to cracks which nucleate internally from inclusions or defects when specimens are subjected to stress amplitudes below the conventional fatigue limit. In case of internal crack nucleation, fatigue strength decreases when the specimen size increases. As reported in [2-

4], the decrement in fatigue strength is physically justifiable by considering the probability of finding inclusions causing failure when the risk volume (region subjected to a stress amplitude above the 90 % of the maximal stress [2]) increases.
Since experimental tests are carried out almost entirely by means of ultrasonic fatigue testing machines, the specimen size and the consequent specimen risk volume are imposed by resonance condition and are generally significantly limited. Experimental tests exploring the gigacycle fatigue properties of materials have been generally carried out by using hourglass shaped specimens with a small diameter (3-6 mm) and a small risk volume. In order to increase the risk volume, dog-bone shaped specimens have been adopted in [2-4]. However, the risk volume of tested specimens (maximum $1000\,\mathrm{mm}^3$) is significantly limited due to the non uniform stress distribution along the specimen length with constant cross section.
The paper proposes a new specimen shape (*Gaussian specimen*) for gigacycle fatigue tests: wave propagation equations are analytically solved in order to obtain a specimen shape characterized by a uniform stress distribution on an extended specimen length and, as a consequence, by a larger risk volume. Dog-bone and Gaussian specimens with different risk volumes are compared through Finite Element Analyses and the range of applicability of the two different specimens in terms of available risk volume is determined. The stress concentration effect due to cross section variation in the specimens is also taken into account in the analyses. Finally, the stress distribution of a dog-bone and a Gaussian specimen with a theoretical risk volume of $5000\,\mathrm{mm}^3$ is experimentally validated through strain gage measurements.

SPECIMEN DESIGN

Specimens adopted for ultrasonic fatigue tests are designed on the basis of equations for wave propagation in an elastic material with the specimen modelled as a one dimension linear elastic body. Stresses are considered uniformly distributed on the cross section and transverse displacements are negligible if compared to longitudinal displacements. In this respect, the displacement amplitude along the specimen, $u(z)$, can be obtained by solving the Webster's equation for a plane wave:

$$u''(z) + \frac{ds(z)/dz}{S(z)} \cdot u'(z) + k^2 \cdot u(z) = 0 \tag{1}$$

where $u'(z) = du(z)/dz$, $u''(z) = d^2u(z)/dz^2$, and $k = 2 \cdot \pi \cdot f / \sqrt{\frac{E_d}{\rho}}$, being f the resonance frequency, and ρ and E_d the specimen material density and dynamic elastic modulus respectively. By inverting and integrating Eq. 1, the specimen cross-section variation for an imposed displacement $u(z)$ is expressed by the following Equation:

$$s(z) = S_0 \cdot e^{-\int \frac{k^2 \cdot u(z) + u''(z)}{u'(z)} dz} \tag{2}$$

where S_0 is a constant of integration depending on the boundary conditions. In order to obtain a uniform stress distribution along the specimen, the displacement distribution must be linear:

$$u_3(z) = A \cdot (kz) + B \tag{3}$$

where $u_3(z)$ denotes the displacement amplitude in part 3 of the Gaussian specimen (Fig. 1) and A and B are constant coefficients. Boundary conditions for ultrasonic specimens require $u_3(L_3) = 0$, where L_3 is half of the total length of part 3 of the specimen (Fig. 1). The constant of integration S_0 is obtained considering that $s(0) = \pi D_2^2 / 4$ for $z = 0$ (Fig. 1); Eq. 2 becomes:

$$s(z) = \pi D_2^2 / 4 \cdot e^{\left(\frac{kL_3}{\sqrt{2}}\right)^2} \cdot e^{-\left(\frac{k(z-L_3)}{\sqrt{2}}\right)^2} \tag{4}$$

Therefore, according to Eq. 4, the specimen cross-section that leads to a uniform stress distribution entails the typical Gaussian shape.

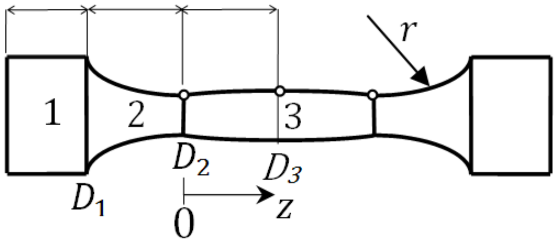

Figure 1: Gaussian specimen.

The total volume of the Gaussian specimen part (i.e., the theoretical risk volume V_{theo}) can be computed by integrating the cross-section of specimen part 3 with respect to z from 0 to L_3 and multiplying it by two:

$$V_{theo} = 2 \cdot \int_0^{L_3} s(z)\,dz = \frac{D_2^2}{k} \cdot \left(\frac{\pi}{2}\right)^{3/2} \cdot e^{\left(\frac{kL_3}{\sqrt{2}}\right)^2} \cdot \mathrm{erf}\left(\frac{kL_3}{\sqrt{2}}\right) \tag{5}$$

where $\mathrm{erf}(\cdot)$ denotes the Error Function (i.e., $\mathrm{erf}(x) = \frac{2}{\sqrt{\pi}} \cdot \int_0^x e^{-t^2} dt$). Eq. 5 allows to compute the length L_3 for desired risk volume, specimen material (i.e., for a chosen value of k) and for the diameter D_2. Part 3 of the specimen is thus completely designed, since D_2, L_3 and k uniquely define the Gaussian specimen part.

In order to determine specimen lengths L_1 and L_2, equations for wave propagation along a straight and catenoidal specimen profile [1], respectively part 1 and part 2 of the specimen (Fig. 1), are solved. The boundary conditions require to have maximum displacement amplitude equal to U_{in} at the interface between the horn and the specimen (i.e., at $z = -(L_1 + L_2)$), continuity of displacement and strain amplitude at the interface between part 1 and part 2 (i.e., at $z = -L_2$) and at the interface between part 2 and part 3 (i.e., at $z = 0$) of the specimen.

A further boundary condition concerning the required stress amplitude in the risk volume is taken into account. Let define the stress amplification factor of the specimen, M_σ, as the ratio between the constant stress amplitude in the Gaussian specimen part, σ, and the maximum stress amplitude in part 1 of the specimen [1], σ_1 (i.e., $M_\sigma = \sigma / \sigma_1 = \sigma / (kU_{in})$). According to the assumption of linear elasticity and introducing the boundary conditions, the stress amplification factor can be expressed as:

$$M_\sigma = \left| N \frac{\beta / k}{\sqrt{1 + \left(\tan(kL_1)\right)^2}} \left(\frac{\cos[\beta L_2] + \tan[\beta L_2]\sin[\beta L_2]}{\tan[\beta L_2] + (\beta / k)(kL_3)} \right) \right| \tag{6}$$

where $N = D_1 / D_2$, being D_1 the diameter of the cylindrical part (part 1 in Fig. 1), $\beta = \sqrt{(kL_2)^2 - \mathrm{acosh}^2(N)} / L_2$ and:

$$kL_1 = \mathrm{atan}\left(-\left(\frac{(\beta / k)(kL_3)\tan(\beta L_2) - 1}{\tan(\beta L_2) / (\beta / k) + (kL_3)} + \frac{\mathrm{acosh}(N)}{kL_2} \sqrt{1 - N^{-2}} \right) \right) \tag{7}$$

According to Eq. 6 and Eq. 7 and for a given value of kL_3, both M_σ and kL_1 depend on the diameter ratio N and on the adimensionalized variable kL_2. Therefore for a chosen resonance frequency, specimen material, diameter ratio N and U_{in} value, the lengths L_2 and L_1 giving a stress amplitude equal to σ in the Gaussian specimen part are obtained and specimen geometry is thus completely defined.

FINITE ELEMENT ANALYSIS: ACTUAL RISK VOLUME AND STRESS CONCENTRATION EVALUATION

Dog-bone and Gaussian specimens with different theoretical risk volumes are tested through Finite Element Analyses (FEA) by using the commercial finite element program ANSYS. Half of the specimen geometrical model is considered in each analysis due to the symmetry of the specimens and eight-node quadrilateral elements (plane 82) with the axisymmetric option are used for the finite element models. The numerical models count for a number of elements ranging from 21200 to 53700 elements. A suitable fillet radius between specimen parts 2 and 3 is considered for the Gaussian specimen model.

Dog-bone and Gaussian specimens are designed considering steel ($E_d = 206\,\text{GPa}$, $\upsilon = 0.29$ and $\rho = 7800\,\text{kg}/\text{m}^3$), a resonance frequency of $20\,\text{kHz}$ (ultrasonic testing machine working frequency), a diameter D_1 equal to $20\,\text{mm}$ and a length L_2 equal to $10.2\,\text{mm}$ (almost equal to the value adopted in [2-4]). The theoretical risk volume is varied by steps of $1000\,\text{mm}^3$: the range considered is within $1000\,\text{mm}^3$ and the maximum theoretical risk volume allowing for an amplification factor M_σ larger than 1.05. The analysis is repeated considering three different diameter ratios N: 1.6, 2 and 2.5.

The actual risk volume and the stress concentration factor are considered in each analysis. The actual risk volume (V_{real}) is the volume of material subjected to stress amplitude larger than the 99% of the maximum stress reached in specimen part 3. An adimensional stress amplitude variation of 0.01 represents a possible tolerance limit for considering the stress amplitude to be almost constant. In order to evaluate the stress concentration effects, the stress concentration factor K_t is conservatively considered in place of the fatigue strength reduction factor K_f. For K_t computation, the nominal stress amplitude is considered equal to the average stress amplitude in the specimen mid-section.

Fig. 2 shows the actual risk volume variation of both types of specimen with respect to the length L_3. According to Fig. 2, the maximum actual risk volume attainable using dog-bone specimens is smaller than $2000\,\text{mm}^3$. An increment of the length with constant cross section gives no effect in the 3 considered case, since the actual risk volume does not change. Gaussian specimens permit to reach larger actual risk volume, up to $8000\,\text{mm}^3$ with a diameter ratio of 1.6. The actual risk volume increases with the length L_3. As expected, for both types of specimen, a small diameter ratio (N = 1.6) permits to obtain the largest actual risk volume.

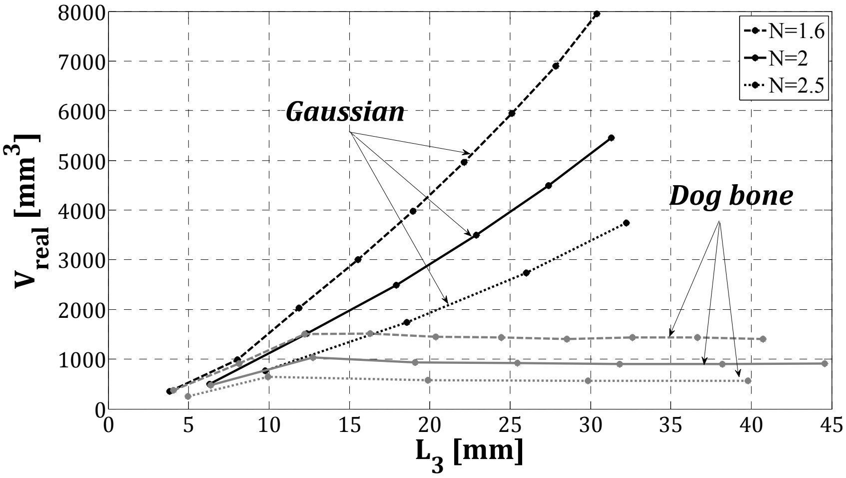

Figure 2: V_{real} of dog-bone and Gaussian specimens with respect to the length L_3.

Fig. 3 reports the percent ratio between the actual risk volume and the theoretical risk volume with respect to the length L_3. According to Fig. 3 and considering dog-bone specimens, the percentage of the theoretical risk volume subjected to almost constant stress reaches a maximum for values of L_3 between $5\,\text{mm}$ and $15\,\text{mm}$. For larger values of the length L_3, the efficiency of the specimens decreases up to 10%. In contrast, considering the Gaussian specimens, the efficiency increases as the length L_3 increases. In general, the highest efficiency is obtained adopting a diameter ratio equal to 2.5 for both types of specimens.

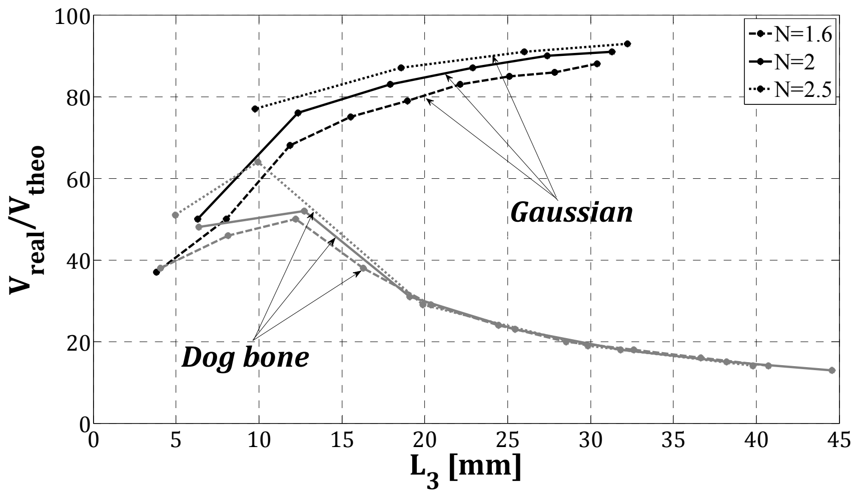

Figure 3: Percent ratio V_{real}/V_{theor} in dog-bone and Gaussian specimens with respect to the length L_3.

Finally, the stress concentration factor is taken into consideration. Fig. 4 shows the variation of K_t with respect to the length L_3. According to Fig. 4, the Gaussian specimens show larger K_t values. Considering dog-bone specimens, there is no stress concentration for L_3 larger than $20\,\text{mm}$. Indeed the stress amplitude decreases considerably in specimen part 3 as the length L_3 increases: therefore the maximum stress due to the cross section variation in specimen part 2 is smaller or equal to the stress reached at the specimen mid-section.

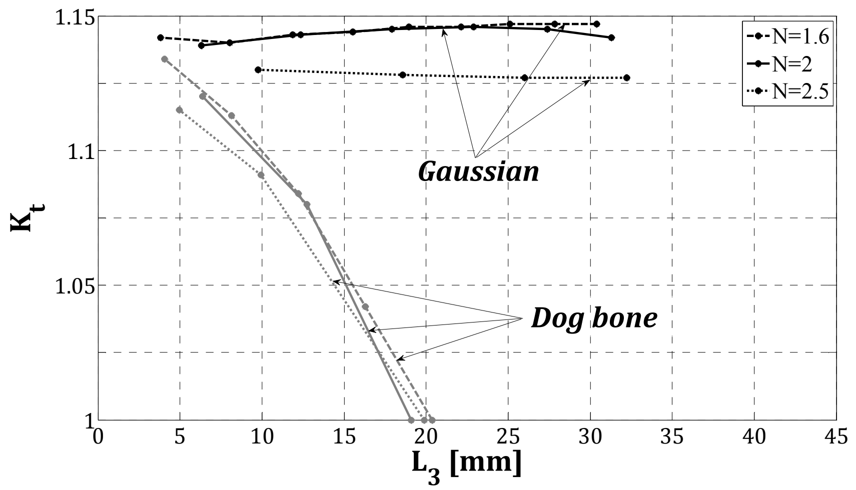

Figure 4: Stress concentration factor of dog-bone and Gaussian specimens with respect to the length L_3

The K_t values of the Gaussian specimens are smaller than 1.15. Taking into account the largest considered diameter ratio ($N = 2.5$), the K_t value reduces up to 1.12. Indeed an increment of the diameter ratio leads to an increment of the fillet radius r (Fig. 1) and, as a consequence, to a reduction of the stress concentration factor. A larger reduction of the stress concentration factor can be obtained by increasing the length L_2. In this respect, a proper choice of the length L_2 and of the diameter ratio allows to design specimens with large actual risk volume and limited K_t value. For instance, a diameter ratio equal to 1.33 and a length L_2 equal to 17.2 mm allows for an actual risk volume larger than $5000\,mm^3$ and a K_t equal to 1.06.

Finally, the adoption of dog-bone specimens is appropriate for very small risk volumes (smaller than $1000\,mm^3$). Gaussian specimens must be adopted for large risk volumes. The length L_2 and the diameter ratio must be properly chosen in order to reduce the stress concentration effects.

EXPERIMENTAL VALIDATION

The stress distribution in the two specimen types is experimentally validated through strain gage measurements. A dog-bone and a Gaussian specimen with a theoretical risk volume of $5000\,mm^3$, diameter ratio $N = 2$ ($D_1 = 20\,mm$) and L_2 equal to 10.2 mm are produced in AISI 1040 carbon steel. Three T-rosettes strain gages (HBM 1-XY31-1.5/350), each with two strain gages connected at half bridge, are used for the evaluation of strain values at the specimen surface. For both specimens, the rosettes are bonded along the specimen central part: the first rosette is bonded at the specimen mid-section, the second rosette at the 70% of L_3 and the third rosette at the 85% of L_3. Fig. 5 shows the specimens after the application of the rosettes.

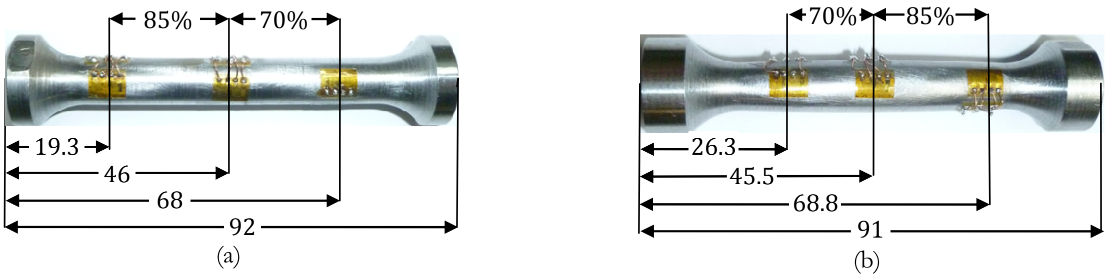

Figure 5: Specimens after application of strain gage rosettes: (a) dog-bone shaped specimen; (b) Gaussian specimen.

A strain gage amplifier (EL-SGA-2/B by Elsys AG) is used for the completion of the Wheatstone bridge of each rosette and for the amplification of the signal. The measurement is acquired at a sample rate of 600 kHz by a National Instruments data acquisition card (PCIe-6363).

An ultrasonic testing machine for fully reversed tension compression tests developed by the authors [5] is used for the test: specimens are subjected to load cycles for 3 seconds. Fig. 6 and 7 show the strain measured at each point normalized by the value detected at the specimen mid-section, σ_{center}.

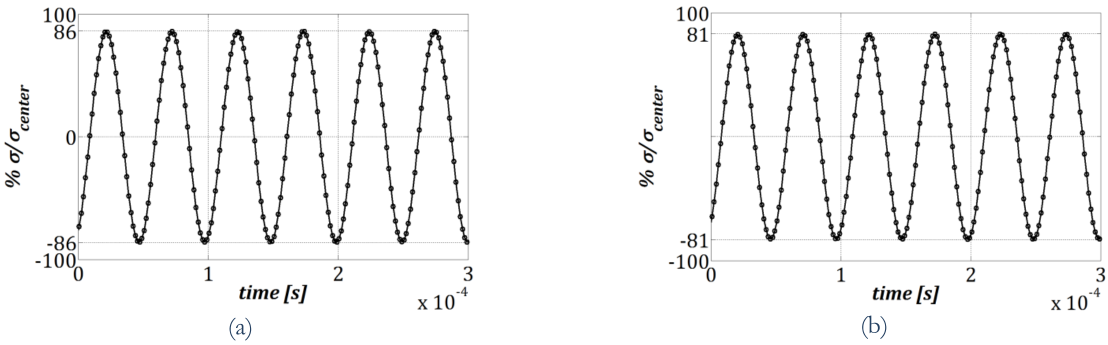

Figure 6: Stress variation measured by strain gage rosettes bonded to the dog-bone shaped specimen: (a) rosette at 70% of L_3; (b) rosette at 85% of L_3.

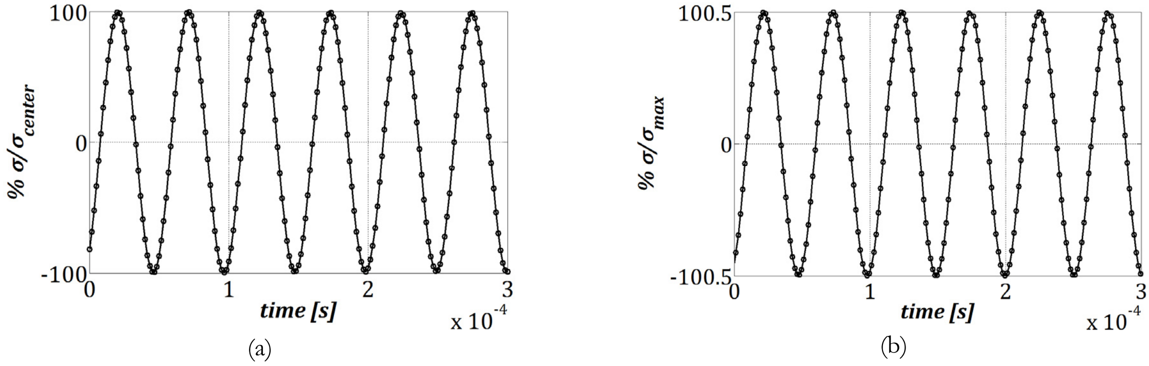

Figure 7: Stress variation measured by strain gage rosettes bonded to the Gaussian specimen: (a) rosette at 70% of L_3; (b) rosette at 85% of L_3.

The acquired signals are fitted with a sine function (for each case, the correlation coefficient is larger than 99.99% and the mean value is equal to zero). As shown in Fig. 6 and 7, the stress amplitude distribution is not uniform for the dog-bone shaped specimen while it is almost uniform for the Gaussian specimen.

Tab. 1 reports a comparison between the stress variation obtained with the finite element analysis (FEA) and the experimental test. According to Tab. 1, the FEA results are included in the experimental confidence intervals. Therefore, it can be concluded that no significant statistical difference exists between FEA and experimental results. It is worth to note that, for the Gaussian specimen, the values larger than the 100% indicate a maximum stress amplitude not reached at the specimen mid-section (Fig. 4).

Analysis type	$z / L_3 = 70$ **%**		$z / L_3 = 85$ **%**	
	Dog-bone	*Gaussian*	*Dog-bone*	*Gaussian*
Finite Element	85.8 %	100.0%	80.2 %	100.2 %
Experimental (95 % confidence interval)	$[85.4;86.5]$ %	$[99.6;100.8]$ %	$[80.1;81.4]$ %	$[100.0;101.1]$ %

Table 1: Comparison between numerical and experimental results: values of the σ / σ_{center} percent ratio.

Note: Confidence intervals are obtained from 180 tests; for each experimental test, stress amplitude is evaluated with a minimum of 1000 data points.

CONCLUSIONS

The proposed Gaussian shape allows to obtain specimens characterized by a very large risk volume. Dog-bone and Gaussian specimens are compared through a Finite Element Analysis. The finite element models are experimentally validated by means of strain gages measurement.

The results show that dog-bone specimens are appropriate only for small risk volumes, while the Gaussian shape allows to design specimens with larger risk volumes (up to $8000\,mm^3$).

The stress concentration effect due to the cross section variation along the specimen is also taken into account. Stress concentration factor is limited for dog-bone specimen. Gaussian specimen shows larger stress concentration factors; an appropriate choice of the length L_2 and of the diameter ratio N allows to design Gaussian specimens with large risk volume and K_t values equal or even smaller than that of the traditional dog-bone specimens.

ACKNOWLEDGMENTS

The authors gratefully acknowledge financial support from the Piedmont Region Industrial Research Project NGP – Bando Misura II.3.

REFERENCES

[1] C. Bathias, P.C. Paris, Gigacycle fatigue in mechanical practice, CRC Dekker, New York (2005).
[2] Y. Furuya, Scripta Materialia, 58 (2008) 1014.
[3] Y. Furuya, Procedia Engineering, 2 (2010) 485.
[4] Y. Furuya, Material Science and Engineering, A 528 (2011) 5234.
[5] D.S. Paolino, M. Rossetto, G. Chiandussi, A. Tridello, In: Proceedings of the 41th AIAS Conference, Vicenza, (2012).